Author/s:
Ziegler, M;Haigh, K;Nguyen, T;Wang, X;Lim, B;Yap, ML;Eddy, EM;Haigh, JJ;Peter, K

Title:
The pulmonary microvasculature entraps induced vascular progenitor cells (iVPCs) systemically delivered after cardiac ischemia-reperfusion injury: Indication for preservation of heart function via paracrine effects beyond engraftment

Date:
2019-02-01

Citation:
Ziegler, M., Haigh, K., Nguyen, T., Wang, X., Lim, B., Yap, M. L., Eddy, E. M., Haigh, J. J. & Peter, K. (2019). The pulmonary microvasculature entraps induced vascular progenitor cells (iVPCs) systemically delivered after cardiac ischemia-reperfusion injury: Indication for preservation of heart function via paracrine effects beyond engraftment. Microcirculation, 26 (2), https://doi.org/10.1111/micc.12493.

DR. MELANIE ZIEGLER (Orcid ID : 0000-0002-6229-5698)

Article type : Original Research

The pulmonary microvasculature entraps induced vascular progenitor cells (iVPCs) systemically delivered after cardiac ischemia-reperfusion injury: Indication for preservation of heart function via paracrine effects beyond engraftment.

Melanie Ziegler[1], Katharina Haigh[2], Thao Nguyen[2], Xiaowei Wang[1,3], Bock Lim[1], May Lin Yap[1], Eleanor M. Eddy[1], Jody J. Haigh[#2], Karlheinz Peter[#1,3]

[1]Atherothrombosis and Vascular Biology, Baker Heart and Diabetes Institute, Melbourne, Australia

[2]Mammalian Functional Genetics Laboratory, Division of Blood Cancers, Australian Centre for Blood Diseases, Monash University, Melbourne, Australia

[3]Department of Medicine, Monash University, Melbourne, Australia

[#]contributed equally as senior authors

Running title: platelet-targeted iVPCs ameliorate I/R injury

This is the author manuscript accepted for publication and has undergone full peer review but has not been through the copyediting, typesetting, pagination and proofreading process, which may lead to differences between this version and the Version of Record. Please cite this article as doi: 10.1111/micc.12493

Corresponding authors:

Karlheinz Peter, MD, PhD

Atherothrombosis and Vascular Biology, Baker Heart & Diabetes Institute

PO Box 6492, Melbourne VIC 3004 Australia

Phone: **+61 3** 85321490; Fax: **+61 3** 85321100

Email: karlheinz.peter@baker.edu.au

Abstract

Objective: Stem cell-based regenerative therapies have been intensively studied with the aim to define an ideal cell type for the treatment of myocardial infarction. We tested systemically delivered, platelet-targeted induced vascular progenitor cells (iVPCs) to study their potential to salvage damaged myocardium after ischemia-reperfusion injury.
Methods: Using a mouse model of ischemia-reperfusion injury, we tested the potential of platelet-targeted iVPCs ($1x10^6$ targ-iVPCs) compared to non-targ-iVPCs and a saline control. Bioluminescence imaging, echocardiography and histological analyses were performed.
Results: 4 weeks after ischemia-reperfusion injury, systemic delivery of targ-iVPCs led to reduced fibrosis and infarct size (PBS: 25.7±3.9 vs targ-iVPC: 18.4±6.6 vs non-targ-iVPC: 25.1±3.7 %I/LV, $p<0.05$), increased neovascularization, and restored cardiac function (PBS: 44.0±4.2 vs targ-iVPC: 54.3±4.5 vs non-targ-iVPC: 46.4±3.8 %EF, $p<0.01$). Cell tracking experiments revealed entrapment of intravenously injected iVPCs in the pulmonary microvasculature in both cell-treated groups.
Conclusions: Systemic delivery of iVPCs after cardiac ischemia-reperfusion injury is limited by pulmonary entrapment of the cells. Nevertheless, targ-iVPCs reduced infarct size, fibrosis, increased neovascularization, and most importantly retained cardiac function. These findings contribute to the mechanistic discussion of cell-based therapy and ultimately identify activated platelet-targeted iVPCs as candidates for cell therapy and also describe cell therapy benefits without the necessity of engrafting.

Keywords: ischemia-reperfusion injury, iVPC, cell delivery, regenerative cell therapy, cell tracking, myocardial infarction

Abbreviations

AAR	Area at risk
CAO	Coronary artery occlusion
DDAB	Dimethyldioctadecylammonium bromide
Dox	Doxycycline
EF	Ejection fraction
GP	Glycoprotein
I	Infarct size
I/R	Ischemia-reperfusion
iPSCs	Induced pluripotent stem cells
iVPCs	Induced vascular progenitor cells
LV	Left ventricular
LVEF	Left ventricular ejection fraction
MI	Myocardial infarction
PBS	Phosphate-buffered saline
Sca-1	Stem cell antigen-1
scFv	Single-chain antibody
TTC	Triphenyltetrazolium chloride

Introduction

Ischemic heart disease such as myocardial infarction (MI) is still the leading cause of mortality and morbidity worldwide.[1] An acute MI is typically caused by rupture of atherosclerotic plaque, leading to thrombotic occlusion of coronary arteries. Following the interrupted blood flow, the affected myocardium builds-up metabolic waste and suffers from a lack of oxygen and nutrient supply. After prolonged ischemia this causes cardiac tissue damage and necrosis. Even if circulation is successfully restored, reperfusion still contributes to final tissue damage of up to 50%.[2] Restoring the damage caused by ischemia-reperfusion (I/R) injury using cell therapy has been extensively investigated. After originally demonstrating great promise in small animal studies, translation of these positive studies to humans has mainly been unsuccessful.[3,4] Therefore, further studies are needed to define cell candidates with the potential to support tissue regeneration not only in small animal

models, but also in bigger primates as well as in humans.[5] In particular, induced pluripotent stem cells (iPSCs) with their indisputable ability to generate cardiomyocytes, provide a potential solution to salvage the infarcted myocardium after I/R injury.[6] In this study we validated the potential of a recently partially reprogrammed and characterised mouse iPSC cell line, termed induced vascular progenitor cells (iVPCs).[7] These cells are not "truly" pluripotent, and maintain cellular memory of their endothelial origin, and as such have developmental potential for revascularisation, as well as other important regenerative properties for cardiac repair.

Delivering intravenously injected therapeutic cells specific to the infarcted myocardium has been a major challenge, therefore most studies injected the cells of interest intracoronarily or intramyocardially.[4] To redirect the iVPCs into the ischemic heart we are using a recently established targeting tool towards activated platelets.[8] Activated platelets have been proven to infiltrate and accumulate directly after I/R injury[9–11] and our generated tandem single-chain antibody (Tand-scFv) shows high affinity binding against the activated glycoprotein (GP)IIb/IIIa ($\alpha_{IIb}/\beta_{IIIa}$; CD41/CD61) on the surface of activated platelets and is therefore an ideal targeting tool to guide intravenously injected stem cell antigen-1 (Sca-1)-positive-cells to the infarcted myocardium. In this study we demonstrate that iVPCs express abundant Sca-1 on their cell surface and Tand-scFv pre-incubated iVPCs have indirect regenerative potential after I/R injury.

Materials and Methods

Mice

NOD.CB17-Prkdc^{scid}/*Arc* mice were purchased from Animal Resources Centre (ARC), Australia and housed by Alfred Medical Research and Education Precinct (AMREP) Animal Services in Melbourne, Victoria, Australia. All experimental work was performed in accordance with the Australian code for the care and use of animals for scientific purposes and approved by the AMREP Animal Ethics Committee (E/1402/2013/B).

Generation, expression, and purification of bispecific Tand-scFv$_{Sca\text{-}1+GPIIb/IIIa}$ and Tand-scFv$_{Sca\text{-}1+Mutant}$

Two different scFvs, activated GPIIb/IIIa-targeted scFv ($scFv_{GPIIb/IIIa}$) and non-targeted scFv ($scFv_{Mutant}$), were fused with $scFv_{Sca\text{-}1}$ and cloned into the pMT vector system as previously described.[8] In brief, both $scFv_{Sca\text{-}1}$-plasmid constructs were produced in *Drosophila melanogaster* Schneider line-2 (S2) cells (Life Technologies) using $CuSO_4$-induced dimethyldioctadecylammonium bromide (DDAB) transfection. Cell supernatant was applied

to a chelating Sepharose fast-flow column to remove the non-specific protein and the copper. Both scFvs contain a 6xHis tag, which was used for further purification with nickel-based metal affinity chromatography (Invitrogen). Specificity and functionality of both Tand-scFvs has been extensively studied and previously described.[8]

Cell culture and preparation

iVPCs cells were isolated and expanded from neonatal lung endothelial cells that were obtained from the previously described R26-iPSC mouse model.[7] Here low passage iVPCs (P 6-8) were cultured in full embryonic stem (ES) cell media + leukemia inhibitory factor (LIF) in the presence of 2ug/ml doxycycline (Dox).[7] 24-48 hours prior to $scFv_{GPIIb/IIIa}$ coupling and IV injection, cells were grown in the absence of Dox to allow OCT4, SOX2, KLF4 and MYC (OSKM) Yamanaka reprogramming factors to be turned off and cells to drift back towards $CD31^+$ channel forming cells.[7]

Expression of Sca-1 on iVPC and binding of Tand-$scFv_{Sca\text{-}1+GPIIb/IIIa}$ and Tand-$scFv_{Sca\text{-}1+Mutant}$ to iVPC by flow cytometry

Expression of Sca-1 receptors has been studied on cultured iVPCs. A single cell suspension of $1.5x10^5$ IVPCs was incubated with Sca-1-PE antibody for 30 min at room temperature (RT). To confirm binding of the bispecific Tand-$scFv_{Sca\text{-}1+GPIIb/IIIa}$ and Tand-$scFv_{Sca\text{-}1+Mutant}$ to the iVPC, 10 µg/ml of the Tand-scFvs was incubated with $1.5x10^5$ IVPCs for 15 min at RT. After washing, cells were stained using Penta-His Alexa Fluor 647 (Qiagen) directed against the 6xHis tag of the bispecific scFvs for 15 min in darkness. Expression of Sca-1 and binding of Tand-$scFv_{Sca\text{-}1+GPIIb/IIIa}$ and Tand-$scFv_{Sca\text{-}1+Mutant}$ were measured using a BD FACS Canto II and analyzed using Flowlogic (Miltenyi Biotec).

Myocardial IR injury and echocardiography

Eight-weeks old, male *NOD*.CB17-Prkdc^{scid}/*Arc* mice were anesthetized using a combination of ketamine HCl (100 mg/kg body weight (wt); Lyppard), xylazine HCl (5 mg/kg body wt; Lyppard), and atropine (1 mg/kg body wt; Pfizer) via intraperitoneal injection. Mice were orally intubated and ventilated using a rodent ventilator (Model 687, Harvard Apparatus), with a tidal volume of 0.18 ml at 120 breaths/min. Mice underwent open-chest surgery to induce left coronary artery occlusion (CAO) for 45 min, followed by reperfusion as previously described.[12] Depending on the treatment group, immediately after reperfusion mice were randomly injected via tail-vein with phosphate-buffered saline (PBS), $1x10^6$ iVPCs pre-incubated with 140 µg/ml Tand-$scFv_{Sca\text{-}1+GPIIb/IIIa}$ (targeted-iVPCs) or Tand-$scFv_{Sca\text{-}1+Mutant}$ (non-targeted-iVPCs).

Mice (n=7–9) underwent serial echocardiography at baseline (1 day before I/R injury), 1 and 4 weeks post-I/R injury using a Vevo 2100 high-resolution small animal scanner (VisualSonics Inc. Toronto, Canada) equipped with a 22–55 MHz MS550D transducer as

described previously.[13] In brief, animals were placed under light sedation (range of 1-2% isoflurane), on the heated VisualSonics imaging station. The temperature of the animal, its heart rate, electrocardiogram, as well as its breathing was monitored. During each echocardiographic examination, the parasternal long-axis of the heart was obtained. Imaging was performed at baseline (before CAO), as well as at weeks 1 and 4 post-I/R injury. Echocardiography, as well as videos and images analyses were performed by a blinded investigator using the VisualSonics imaging software (VisualSonics Inc. Toronto, Canada). The ejection fraction (EF) was calculated using the Simpson method from the parasternal long-axis B-mode images. After 28 days, mice were euthanized for Evans blue/ triphenyltetrazolium chloride (TTC) staining as described below and histological analysis.

Evans Blue/TTC staining

Mice were anaesthetized 4 weeks post-I/R and the ischemic area (area at risk (AaR)) and infarcted area (infarct size (I)) was assessed by Evans Blue/TTC staining. The LAD was re-ligated with the original suture and 4% Evans Blue (AppliChem) was injected to stain the perfused regions blue. The heart was then cut into 6 transversal slices and stained with 1% TTC (Sigma) for 10 min at 37℃. TTC turns the metabolically active areas red, while the infarcted necrotic myocardial tissue remains white (I). Thereafter, the heart slices were photographed on both sides using a digital camera. A blinded researcher determined the infarct sizes by quantitative morphometric planimetry using an image analysis software program.

Histology

Mice were euthanized after 28 days, the hearts were harvested, fixed in 4% paraformaldehyde (PFA), embedded in paraffin, followed by cutting into sections 6 µm thick. Four defined heart sections for each mouse were stained using a Masson's Trichrome Staining Kit (Australian Biostain P/L) according to the manufacturer's protocol. Slides were imaged on an Olympus BX50F-3 microscope (Olympus Optical Co., Japan) using 12.5x magnification. Blue-stained collagen distribution was measured as the percentage area of the total left ventricle using ImageJ v1.48.

Immunohistochemistry

Two random cardiac sections for each mouse were immunostained using rat anti-mouse CD31 monoclonal antibody (0.3 µg/ml, BD Pharmingen) and a corresponding isotype control antibody. A rat-biotinylated secondary antibody (Vector Laboratories) was applied for 30 min at RT. Immunostaining of cardiac sections was performed with a streptavidin–biotin–immunoperoxidase method (Vectostatin ABC-Peroxidase and diaminobenzidine; Vector Laboratories) as per the manufacturer's protocol. Samples were imaged on an Olympus BX50F-3 microscope using 200x magnification. Vessels have been defined by CD31-positive brown staining. The numbers of $CD31^+$-vessels were quantified from six random

areas from the infarct zone as well as from the non-infarct zone of each heart sample and were measured within a defined tissue area (mm^2).

In vivo imaging system (IVIS) to study cell tracking

iVPCs cells were cultured in the presence of 2ug/ml Dox prior to the cell tracking experiment. 24 h prior to MI-inducing surgery, mice were treated with drinking water containing 2mg/ml Dox, to ensure that Luciferase is continuously expressed in iVPCs. Mice underwent MI-inducing surgery by CAO for 45 min. In the meantime, iVPC cells were incubated with 140 µg/ml Tand-$scFv_{Sca\text{-}1+GPIIb/IIIa}$ or Tand-$scFv_{Sca\text{-}1+Mutant}$ for 15 min at RT. Immediately after reperfusion, $1x10^6$ cells/mouse were injected, allowed to circulate for 3 h and D-Luciferin (150ug/g BW, Perkin Elmer) was IV injected 10 min prior to euthanasia. 3 h after reperfusion, mice were euthanized, the organs were perfused and collected in PBS, and imaged using an IVIS Lumina XRMS system (Perkin Elmer).

Statistical analysis

All experiments were performed at least in 3 independent assays (n=3) unless otherwise noted. I/R injury-inducing surgery was performed on n=9 mice per treatment group. Data were statistically analyzed using one- or two-way repeated-measures ANOVA. *Post hoc*, a Bonferroni's multiple comparisons test was used. P values of less than 0.05 were considered statistically significant. All results are expressed as mean ± standard deviation (SD).

Results

Expression of Sca-1 on iVPCs and binding of the bispecific Tand-$scFv_{Sca\text{-}1+GPIIb/IIIa}$ and the corresponding control single-chain antibody Tand-$scFv_{Sca\text{-}1+Mutant}$ to iVPCs

Our group has previously developed and characterized a tandem single-chain antibody Tand-$scFv_{Sca\text{-}1+GPIIb/IIIa}$ to specifically deliver intravenously injected Sca-1 positive cells to activated platelets, which accumulate specifically to the ischemic tissue of the heart soon after I/R injury.[8] As iVPCs might be a promising therapeutic cell for cardiac regeneration, we tested the expression of Sca-1 on the iVPC surface using flow cytometry. Incubating the iVPCs with a Sca-1-PE antibody showed high expression of Sca-1 on iVPCs compared to the unstained control iVPCs (Figure 1 A). Furthermore, binding of the Tand-$scFv_{Sca\text{-}1+GPIIb/IIIa}$ as well as the Tand-$scFv_{Sca\text{-}1+Mutant}$ control antibody to iVPC, was demonstrated using flow cytometry (Figure 1 B+C).

Targ-iVPC preserves left ventricular cardiac function after I/R injury

Having confirmed that iVPCs do express Sca-1 on their surface and that Tand-$scFv_{Sca\text{-}1+GPIIb/IIIa}$ specifically binds to the iVPCs in vitro, we hypothesized that iVPCs incubated with Tand-$scFv_{Sca\text{-}1+GPIIb/IIIa}$ (so called targ-iVPC) accumulate in the myocardium post I/R injury

and may have beneficial effects after myocardial infarction. This hypothesis was tested in a mouse model of cardiac I/R injury. *NOD*.CB17-Prkdc^{scid}/*Arc* mice underwent CAO for 45 min followed by reperfusion. Directly after reperfusion, mice were injected with either PBS, 1x10^6 targ-iVPC or 1x10^6 iVPCs pre-incubated with Tand-scFv$_{Sca\text{-}1+Mutant}$ (non-targ-iVPC). Ejection fraction (EF) was analyzed using Simpson's method from the parasternal long-axis B-mode images at baseline (1 day prior surgery) as well as weeks 1 and 4 post-I/R injury. Baseline EF was similar between the groups (PBS: 53.3 ± 3.5 %EF versus (vs) targ-iVPC: 55.4 ± 5.1 %EF vs non-targ-iVPC: 53.5 ± 5.5 %EF; Figure 2 A). The trend toward better EF was observed for the targ-iVPC treated group at week 1 post-I/R (PBS: 44.7 ± 4.1 vs targ-iVPC: 52.8 ± 4.7 vs non-targ-iVPC: 47.7 ± 4.8 %EF). In week 4, EF of mice treated with targ-iVPCs has been preserved compared to mice treated with non-targ-iVPCs or PBS (PBS: 44.0 ± 4.2 vs targ-iVPC: 54.3 ± 4.5 vs non-targ-iVPC: 46.4 ± 3.8 %EF; Figure 2 B). Respiration rate and heart rate have been monitored at baseline and at week 4 post-I/R and did not reveal treatment differences (Figure 2 C+D). Taken together, platelet-targeted cell therapy using targ-iVPC preserves cardiac function after I/R injury.

Administration of targ-iVPC ameliorates cardiac remodeling after I/R injury

Four weeks after I/R injury, histological evaluation of infarct size was assessed using Evans blue/TTC staining. Targ-iVPC treated mice showed a significant reduction in infarct size (I)/ left ventricle (LV) ratio as well as to area at risk (AaR) ratio, compared to PBS and non-targ-iVPC treated mice (PBS: 25.7 ± 3.9 vs targ-iVPC: 18.4 ± 6.6 vs non-targ-iVPC: 25.1 ± 3.7 %I/LV; Figure 3 A+B). This decrease in infarct size was accompanied by reduced fibrotic areas (as assessed by Masson's trichrome staining) in mice treated with targ-iVPC, compared to mice treated with PBS or non-targ-iVPC (PBS: 13.9 ± 4.3 vs targ-iVPC: 8.4 ± 3.4 vs non-targ-iVPC: 14.1 ± 4.1 % collagen content/LV; Figure 3 C+D). Furthermore, neovascularization was analyzed by immunohistochemistry using an anti-CD31 antibody. The average vessel density in the infarct zone was significantly enhanced in mice treated with targ-iVPC in comparison to mice treated with PBS or non-targ-iVPC (PBS: 479 ± 83 vs targ-iVPC: 710 ± 99 vs non-targ-iVPC: 519 ± 152 CD31$^+$-vessels/mm^2; Figure 4 A+B). There was no change in the average vessel density observed in the non-infarcted zone throughout all three treatment groups (Figure 4 C+D).

In summary, administration of targ-iVPC decreases infarct size as well as fibrosis, and enhances neovascularization 4 weeks after I/R injury.

Cell tracking of targ-iVPC reveals accumulation of iVPCs in the lung after I/R injury

To investigate the fate of the delivered cells as well as the underlying cellular mechanisms of the demonstrated functional improvement in the myocardium, cell tracking experiments have

been performed. The administered iVPCs have the big advantage that they have a Dox-inducible luciferase cassette included in the genome and are therefore suitable for cell tracking experiments.[7] This internal ribosome entry site-enhanced green fluorescent protein (IRES-EGFP)-Luciferase reporter is downstream of the tet(o) inducible OSKM reprogramming factors and its expression can be controlled by doxycycline administration. However, only living iVPCs catalyze luciferin and are detectable with the luminescence scans, while dead cells or released exosomes will not catalyze luciferin and therefore they are undetectable in this experimental setting.

After I/R injury, mice were intravenously injected with targ-iVPC or non-targ-iVPC. 10 min prior to the IVIS scan, luciferin was injected and catalyzation by luciferase from the iVPCs was assessed. As a negative control, organs from a healthy mouse without cell injection were collected. As a positive control, iVPCs injected intracardially after the heart collection were used. Luminescence scans, using an IVIS Lumina XRMS scanner, were performed from the heart, blood, and lung 3 h after cell injection (Figure 5). IVIS scan of the heart showed only the presence of vital iVPCs when injected intracardially while intravenously injected targ-iVPC as well as non-targ-iVPC were not measurable in the myocardium 3 h post I/R injury (Figure 5A). No relevant luminescence signal was detected in the blood (Figure 5B). The scan of the lungs revealed that intravenously injected iVPCs, targ-iVPCs as well as non-targ-iVPCs, gets entrapped in the microcirculation of the lung (Figure 5C). Furthermore, a biodistribution analysis was performed by scanning the spleen, heart, lung, liver, kidney and femur (Figure 6). This scan revealed and confirmed that the vital cells are trapped in the lungs while all other scanned organs throughout all treatment groups showed no significant change in luminescence levels. Taken together, these data demonstrate that intravenously injected iVPCs get entrapped in the microcirculation of the lungs.

Discussion

We systematically investigated a novel cell therapeutic strategy for cardiac ischemia-reperfusion injury. First, we demonstrated the expression of Sca-1 on iVPCs and proved successful targeting of iVPCs with the Tand-scFv$_{Sca\text{-}1+GPIIb/IIIa}$. Next, we tested iVPCs in a activated platelet-targeted approach as a cell therapy strategy post-MI. Systemic delivery of Tand-scFv$_{Sca\text{-}1+GPIIb/IIIa}$ pre-incubated iVPCs via intravenous injection showed reduced infarct size, decreased fibrosis, enhanced vessel density, and, most importantly, restored cardiac LV function four weeks after I/R injury. Interestingly, cell tracking studies revealed that targ-

iVPCs were entrapped in the microcirculation of the lungs and were not found integrated into blood vessels in the area of the infarcted myocardium.

Intravenous cell injection has been described to have several advantages such as non-invasive, cost-effective as well as a uniform distribution of the injected cells in the damaged heart tissue.[14] However, as shown in the herein presented study and other cell tracking studies, cell size is a major limitation of systemic cell delivery.[15–17] Mouse stem and progenitor cells have an average size of 20–45 µm compared to circulating white blood cells of only 4–9 µm.[18] However, the capillaries in the lung measure about 5–8 µm in diameter.[19] This might be the main reason why stem and progenitor cells are easily trapped in the pulmonary microvasculature after systemic cell infusion and might explain how enhanced cell delivery with low entrapment in the lungs was achieved in our initial platelet-targeted study when we pre-incubated peripheral blood mononuclear cells (PBMCs) with the Tand-scFv$_{Sca-1+GPIIb/IIIa}$.[8] To avoid the limitation of the microvasculature, targ-iVPCs could be injected intramyocardially. This was performed in a previous study by Yin et al. with a similar cell line and the authors presented engraftment of the cells into the blood vessels of the myocardium, stimulated coronary collateral growth, and improved cardiac function after repetitive ischemia in rats post intracardial cell transplantation of iVPCs.[20]

Despite the pulmonary entrapment of the targ-iVPCs and the lack of iVPC delivery specific to the infarcted myocardium, significant cardiac benefits have still been observed when mice were treated with targ-iVPCs compared to non-targ-iVPCs or PBS. We hypothesize that these effects might be explained by paracrine signaling of exosomes/microparticles, which are shed/released from the entrapped donor cells, rather than by cell transdifferentiation and long-term integration into the ischemic myocardium.[21] Stress-induced cells are known to shed/release increased amounts of exosomes containing different cytokines, chemokines and growth-factors. These exosomes might still be covered with the Tand-scFv$_{Sca-1+GPIIb/IIIa}$ and this might guide the exosomes specifically to the infarcted myocardium where they support cardiac-repair mechanisms after I/R injury by releasing several growth factors, chemokines and cytokines. These released factors can either protect the heart tissue directly, or stimulate progenitor cells and thus promote cardiac repair indirectly. There is a growing body of evidence that exosomes secreted by various cell types have significant beneficial effects after myocardial I/R injury.[22] Further research is required to prove the entrapped targ-iVPCs are indeed able to release Tand-scFv$_{Sca-1+GPIIb/IIIa}$ coated exosomes and home to the ischemic myocardium. However, the herein performed cell tracking experiments, using the described luciferin-luciferase reaction, only detect intact/live cells while released exosomes are undetectable in this experimental setting.

With regards to the exosomes as beneficial transmitter, there is a growing body of evidence that exosomes alone, collected from either stress-induced PBMCs or mesenchymal stem cells (MSCs), have high regenerative capacity, including enhancement of angiogenesis, and have the potential to modify the inflammatory response after an ischemic event and thus restore cardiac function.[23–25] Although further research is required to fully delineate the underlying mechanisms of injected exosomes, a wide array of signaling pathways have been implicated in paracrine-mediated cardiac repair.[26]

In conclusion, Tand-scFv$_{Sca\text{-}1+GPIIb/IIIa}$ pre-incubated iVPCs might be too large for intravenous cell injection and can be entrapped in the pulmonary microvasculature. However, using targeted-iVPC exosomes might be a solution to harness the cardiac benefits of the iVPCs after I/R injury while avoiding entrapment of the cells in the microcirculation of the lungs due to their size.

Limitations

This study used immunosuppressive *NOD*.CB17-Prkdc^{scid}/*Arc* mice, which is a suitable mouse strain to study cell injection experiments. However, this strain shows an attenuation of the inflammatory response after I/R injury. A further limitation of the study is the assessment of infarct size and area at risk using Evans Blue/TTC staining 4 weeks post-I/R injury. Although, this is a well-established and widely used method, the formation of collateral vessels after I/R injury might slightly modify the area at risk.[27]

Perspectives

The presented study demonstrates the regenerative potential of activated platelet-targeted-iVPCs after cardiac I/R injury. However, our study also highlights the limitations of intravenous iVPC injection caused by the entrapment of the injected cells in the pulmonary microvasculature. Our data contribute to the controversial discussion of cell therapy after myocardial infarction in two different directions of further study. Firstly, activated platelet targeted-iVPCs are beneficial after cardiac I/R injury. Secondly, improved cardiac function after I/R injury can be achieved by cells without engraftment into the myocardium.

Acknowledgements

This work was supported by the National Health and Medical Research Council, the German Research Foundation (MZ 1479/1-1), and the National Heart Foundation of Australia (XW100517).

Author contributions: MZ, JJH and KP designed the study. MZ, KH, XW, BL, MLY and EME conducted the experiments and analyzed the data. MZ, JJH and KP wrote the paper. JJH and KP administrated the project.

Conflict of Interest: KP is an inventor on patents describing activated platelet–targeting recombinant antibodies. The other authors have declared that no conflict of interest exists.

References

1. World Health Organization. The top 10 causes of death in the world, 2000 and 2012. *World Health Organ* 2014;

2. Yellon DM, Hausenloy DJ. Myocardial reperfusion injury. *N Engl J Med* 2007;**357**:1121–1135.

3. Bolli R, Ghafghazi S. Stem cells: Cell therapy for cardiac repair: what is needed to move forward? *Nat Rev Cardiol* 2017;**14**:257–258.

4. Fisher SA, Doree C, Mathur A, Martin-Rendon E. Meta-analysis of cell therapy trials for patients with heart failure. *Circ Res* 2015;**116**:1361–1377.

5. Dixit P, Katare R. Challenges in identifying the best source of stem cells for cardiac regeneration therapy. *Stem Cell Res Ther* 2015;**6**:26.

6. Blin G, Nury D, Stefanovic S, Neri T, Guillevic O, Brinon B, Bellamy V, Rücker-Martin C, Barbry P, Bel A, Bruneval P, Cowan C, Pouly J, Mitalipov S, Gouadon E, Binder P, Hagège A, Desnos M, Renaud J-F, Menasché P, Pucéat M. A purified population of multipotent cardiovascular progenitors derived from primate pluripotent stem cells engrafts in postmyocardial infarcted nonhuman primates. *J Clin Invest* 2010;**120**:1125–1139.

7. Haenebalcke L, Goossens S, Dierickx P, Bartunkova S, D'Hont J, Haigh K, Hochepied T, Wirth D, Nagy A, Haigh JJ. The ROSA26-iPSC Mouse: A Conditional, Inducible, and Exchangeable Resource for Studying Cellular (De)Differentiation. *Cell Rep* 2013;**3**:335–341.

8. Ziegler M, Wang X, Lim B, Leitner E, Klingberg F, Ching V, Yao Y, Huang D, Gao X-M, Kiriazis H, Du X-J, Haigh JJ, Bobik A, Hagemeyer CE, Ahrens I, Peter K. Platelet-Targeted Delivery of Peripheral Blood Mononuclear Cells to the Ischemic Heart

Restores Cardiac Function after Ischemia-Reperfusion Injury. *Theranostics* 2017;**7**:3192–3206.

9. Xu Y, Huo Y, Toufektsian MC, Ramos SI, Ma Y, Tejani AD, French BA, Yang Z. Activated platelets contribute importantly to myocardial reperfusion injury. *Am J Physiol Heart Circ Physiol* 2006;**290**:H692-9.

10. Ziegler M, Alt K, Paterson BM, Kanellakis P, Bobik A, Donnelly PS, Hagemeyer CE, Peter K. Highly Sensitive Detection of Minimal Cardiac Ischemia using Positron Emission Tomography Imaging of Activated Platelets. *Sci Rep* 2016;**6**:38161–38161.

11. Elverfeldt D von, Maier A, Duerschmied D, Braig M, Witsch T, Wang X, Mauler M, Neudorfer I, Menza M, Idzko M, Zirlik A, Heidt T, Bronsert P, Bode C, Peter K, Zur Muhlen C von. Dual-contrast molecular imaging allows noninvasive characterization of myocardial ischemia/reperfusion injury after coronary vessel occlusion in mice by magnetic resonance imaging. *Circulation* 2014;**130**:676–687.

12. Ziegler M, Elvers M, Baumer Y, Leder C, Ochmann C, Schonberger T, Jurgens T, Geisler T, Schlosshauer B, Lunov O, Engelhardt S, Simmet T, Gawaz M. The bispecific SDF1-GPVI fusion protein preserves myocardial function after transient ischemia in mice. *Circulation* 2012;**125**:685–696.

13. Ziegler M, Hohmann JD, Searle AK, Abraham M-K, Nandurkar HH, Wang X, Peter K. A single-chain antibody-CD39 fusion protein targeting activated platelets protects from cardiac ischaemia/reperfusion injury. *Eur Heart J* 2018;**39**:111–116.

14. Lalit PA, Hei DJ, Raval AN, Kamp TJ. Induced pluripotent stem cells for post-myocardial infarction repair: remarkable opportunities and challenges. *Circ Res* 2014;**114**:1328–1345.

15. Barbash IM, Chouraqui P, Baron J, Feinberg MS, Etzion S, Tessone A, Miller L, Guetta E, Zipori D, Kedes LH, Kloner RA, Leor J. Systemic delivery of bone marrow-derived mesenchymal stem cells to the infarcted myocardium: feasibility, cell migration, and body distribution. *Circulation* 2003;**108**:863–868.

16. Aicher A, Brenner W, Zuhayra M, Badorff C, Massoudi S, Assmus B, Eckey T, Henze E, Zeiher AM, Dimmeler S. Assessment of the tissue distribution of transplanted human endothelial progenitor cells by radioactive labeling. *Circulation* 2003;**107**:2134–2139.

17. Hofmann M, Wollert KC, Meyer GP, Menke A, Arseniev L, Hertenstein B, Ganser A, Knapp WH, Drexler H. Monitoring of bone marrow cell homing into the infarcted human myocardium. *Circulation* 2005;**111**:2198–2202.

18. Hoogduijn MJ, Beukel JC van den, Wiersma LC, Ijzer J. Morphology and size of stem cells from mouse and whale: observational study. *BMJ* 2013;**347**:f6833.

19. Townsley MI. Structure and composition of pulmonary arteries, capillaries and veins. *Compr Physiol* 2012;**2**:675–709.

20. Yin L, Ohanyan V, Pung YF, DeLucia A, Bailey E, Enrick M, Stevanov K, Kolz CL, Guarini G, Chilian WM. Induction of Vascular Progenitor Cells From Endothelial Cells Stimulates Coronary Collateral GrowthNovelty and Significance. *Circ Res* 2012;**110**:241–252.

21. Sahoo S, Losordo DW. Exosomes and cardiac repair after myocardial infarction. *Circ Res* 2014;**114**:333–344.

22. Barile L, Milano G, Vassalli G. Beneficial effects of exosomes secreted by cardiac-derived progenitor cells and other cell types in myocardial ischemia. *Stem Cell Investig* 2017;**4**.

23. Lichtenauer M, Mildner M, Hoetzenecker K, Zimmermann M, Podesser BK, Sipos W, Berenyi E, Dworschak M, Tschachler E, Gyongyosi M, Ankersmit HJ. Secretome of apoptotic peripheral blood cells (APOSEC) confers cytoprotection to cardiomyocytes and inhibits tissue remodelling after acute myocardial infarction: a preclinical study. *Basic Res Cardiol* 2011;**106**:1283–1297.

24. Ranganath SH, Levy O, Inamdar MS, Karp JM. Harnessing the mesenchymal stem cell secretome for the treatment of cardiovascular disease. *Cell Stem Cell* 2012;**10**:244–258.

25. Mildner M, Hacker S, Haider T, Gschwandtner M, Werba G, Barresi C, Zimmermann M, Golabi B, Tschachler E, Ankersmit HJ. Secretome of peripheral blood mononuclear cells enhances wound healing. *PLoS One* 2013;**8**:e60103.

26. Gnecchi M, Zhang Z, Ni A, Dzau VJ. Paracrine mechanisms in adult stem cell signaling and therapy. *Circ Res* 2008;**103**:1204–1219.

27. Zhang H, Faber JE. De-novo Collateral Formation Following Acute Myocardial Infarction: Dependence on CCR2+ Bone Marrow Cells. *J Mol Cell Cardiol* 2015;**87**:4–16.

Figure legends

Figure 1: Expression of Sca-1 on iVPCs and in vitro binding test of Tand-scFv$_{Sca-1+GPIIb/IIIa}$ and Tand-scFv$_{Sca-1+Mutant}$. A) Representative histograms show high surface expression of Sca-1 on iVPCs measured using a commercial Sca-1-PE antibody (green), as well as high affinity binding of **B)** Tand-scFv$_{Sca-1+GPIIb/IIIa}$ (red) and **C)** Tand-scFv$_{Sca-1+Mutant}$ (blue) to iVPCs.

Figure 2: Preserved left ventricular ejection fraction in mice treated with targeted-iVPC after I/R injury. **A)** Mice treated with targ-iVPC show a better preservation of ejection fraction compared to non-targ-iVPC or PBS-treated mice after I/R injury. **B)** Four weeks post-MI, administration of targ-iVPC restored ejection fraction compared to administration of non-targ-iVPC or PBS, **p<0.01, ***p<0.001, mean ± SD, n=7-9. **C)** Heart rate was analyzed between the three experimental groups at baseline and at week 4 post-I/R. No difference between the treatment groups was observed, n=7-9. **D)** Respiration rate was monitored at baseline and at week 4 post-I/R injury and did not differ between the treatment groups, n=7-9.

Figure 3: Reduced infarct size and fibrosis in mice treated with targeted-iVPC after I/R injury. **A)** Representative images of Evans blue/TTC staining 28 days post I/R injury (scale bar 1 mm). **B)** Quantitative analysis of Evans blue/TTC staining shows a significant decrease in infarct size normalized to left ventricle (LV) as well as to area at risk (AaR) in mice treated with targ-iVPC compared to both control groups. **C+D)** Cardiac sections were stained using Masson's Trichrome. Collagen was stained blue and muscle was counterstained (red). **C)** Representative images of Masson's trichrome staining is shown (scale bar 1 mm, magnification 12.5x). **D)** Quantitative analysis of fibrosis within the left ventricle (LV) is shown. Administration of targ-iVPC caused a significant decrease in fibrosis measured by collagen content, *p<0.05, mean ± SD, n=7-9.

Figure 4: Increase in neovascularization within the infarcted tissue in mice treated with targeted-iVPC after I/R injury. Four weeks post-I/R, cardiac sections were immunostained with anti-CD31 antibody. Blood vessels were stained brown and cell nuclei were counterstained with haematoxylin (blue). **A)** Representative images of CD31 staining within the infarct area 28 days post I/R injury (scale bar: 50 µm, magnification: 200x). **B)** Quantitative analysis of neovascularisation in a defined tissue area ($CD31^+$-vessels/mm^2) is shown. Treatment of targ-iVPC significantly increased neovascularization, as compared to PBS or non-targ-iVPC treated mice within the infarcted area. **C)** Representative images of $CD31^+$-vessel staining within the non-infarct area 4 weeks post I/R injury (scale bar: 50 µm, magnification: 200x). **D)** Quantitative analysis of $CD31^+$-vessels/mm^2 is shown and an equal amount of $CD31^+$-vessels within the non-infarcted area has been quantified throughout all three treatment groups. Data are represented as mean ± SD, n=7-9.

Figure 5: Entrapment of intravenously injected iVPCs in the lung post-I/R injury. Mice underwent 45 min of ischemia followed by reperfusion and iVPC injection. 3 h after reperfusion, mice were intravenously injected with luciferin, organs were harvested 10 min later and an IVIS luminescence scan was performed. **A)** Representative IVIS image shows accumulation of only intracardially injected iVPCs within the heart compared to intravenously injected targ-iVPC as well as non-targ-iVPC, n=3. **B)** Representative IVIS image of blood samples displayed cell clearance in the blood throughout all treatment groups, n=3. **C)** Representative scan of the lung shows entrapment of targ-iVPC and non-targ-iVPC in the microcirculation of the lung, n=3, I) healthy; II) iVPC intracardial injected; III) targ-iVPC; and IV) non-targ-iVPC.

Figure 6: Biodistribution of iVPCs throughout heart, spleen, liver, lung, femur and the kidney. Mice underwent 45 min of ischemia followed by reperfusion and iVPC injection. 3 h after reperfusion, mice were intravenously injected with luciferin, organs were harvested 10 min later and an IVIS luminescence scan was performed. Representative IVIS image showed accumulation of intravenously injected targ-iVPC as well as non-targ-iVPC in the lungs (L), while no relevant luminescence signal was detected in the spleen (S), heart (H), liver (Li), kidney (K) and femur (F), n=3, I) healthy; II) iVPC intracardial injected; III) targ-iVPC; and IV) non-targ-iVPC.

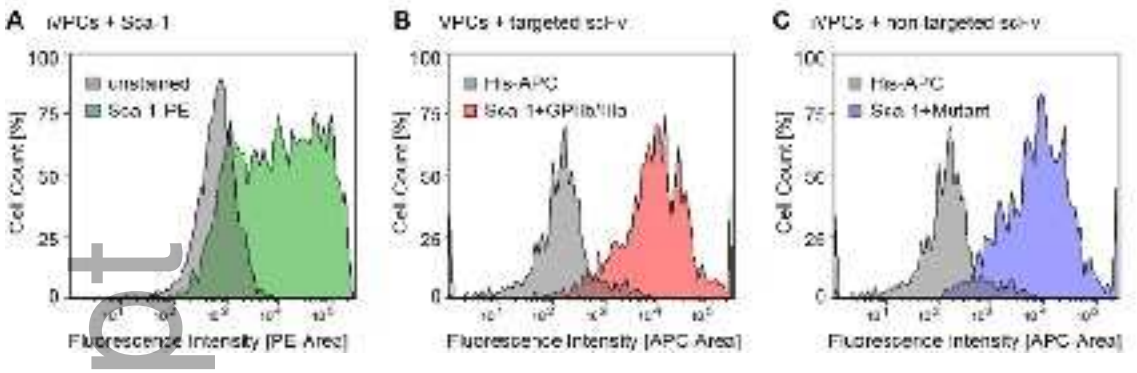

micc_12493_f1.png

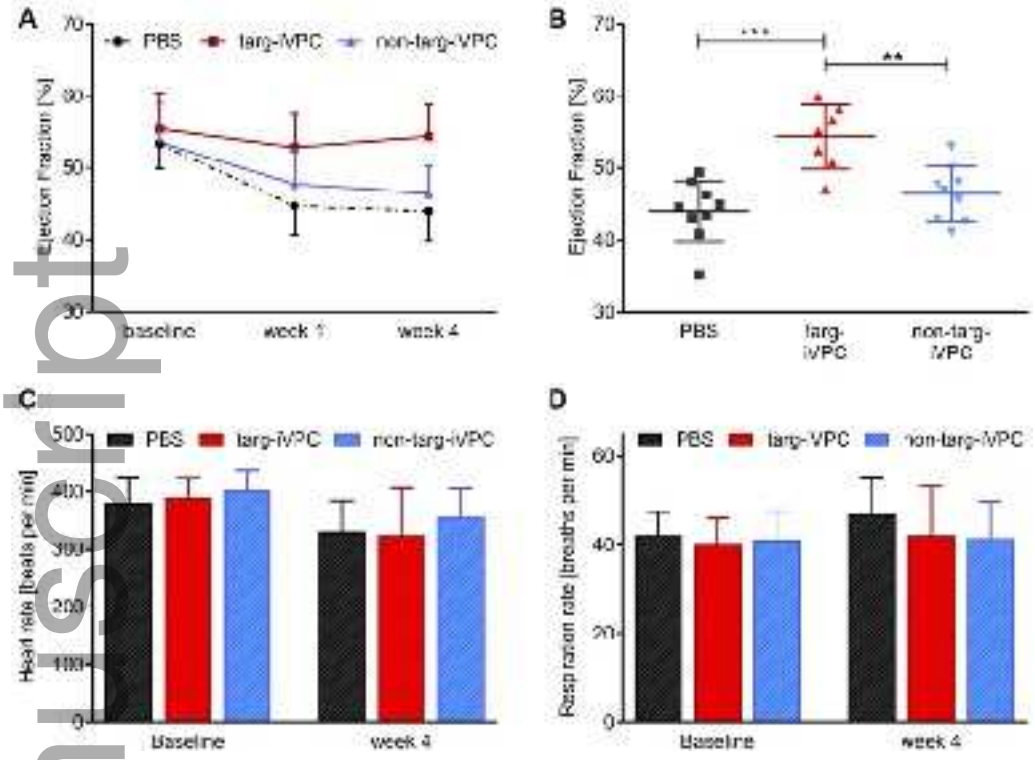

micc_12493_f2.jpg

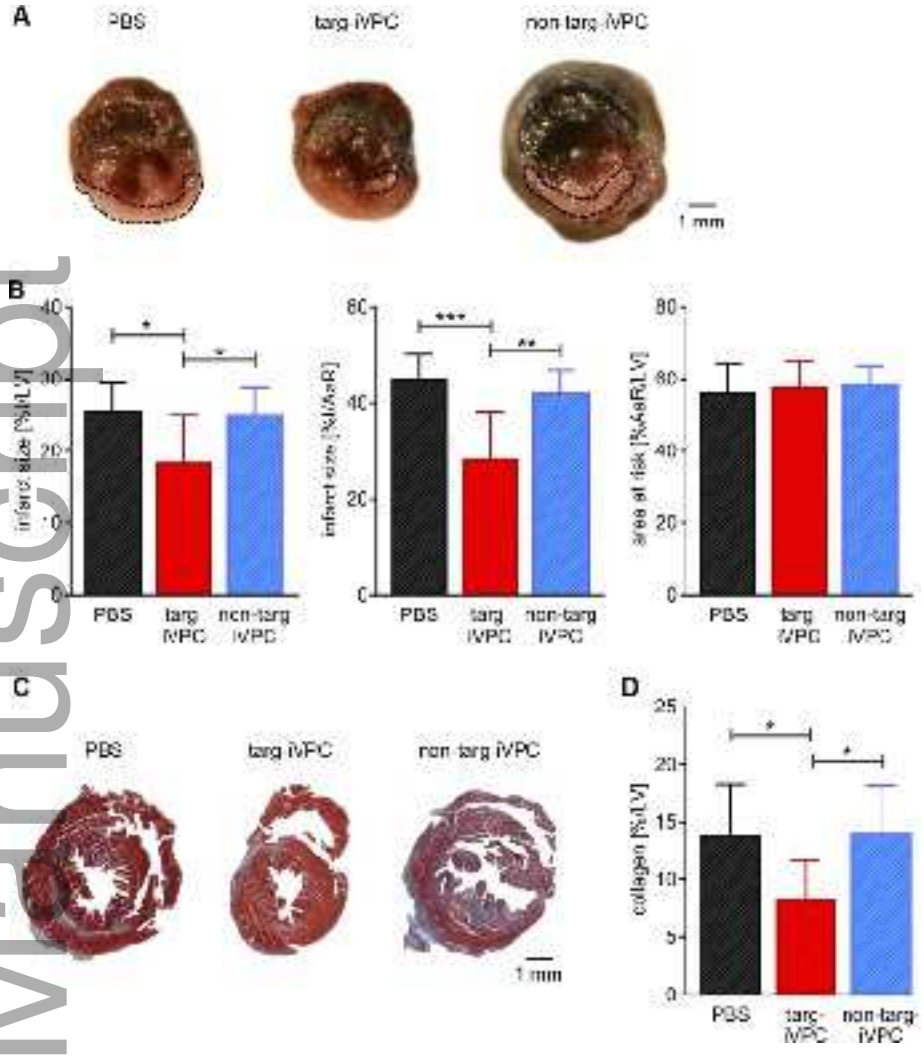

micc_12493_f3.png

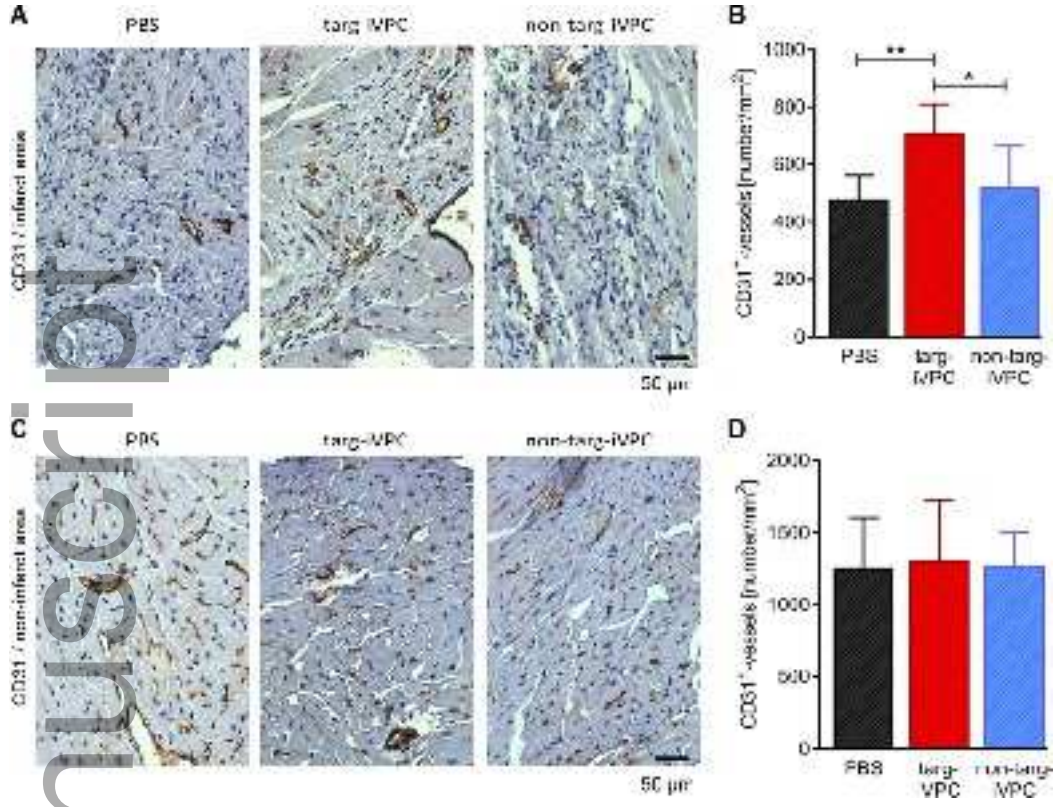

micc_12493_f4.png

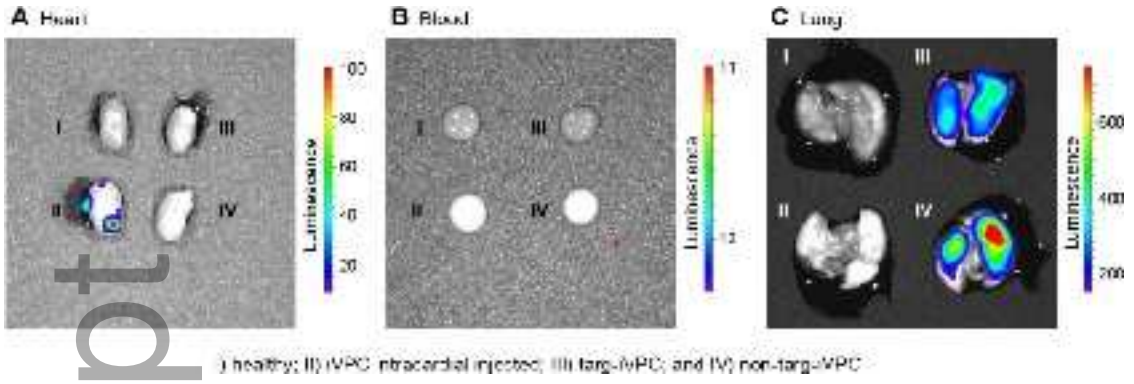

I) healthy; II) rVPC intracardial injected; III) targ-rVPC; and IV) non-targ-rVPC

micc_12493_f5.png

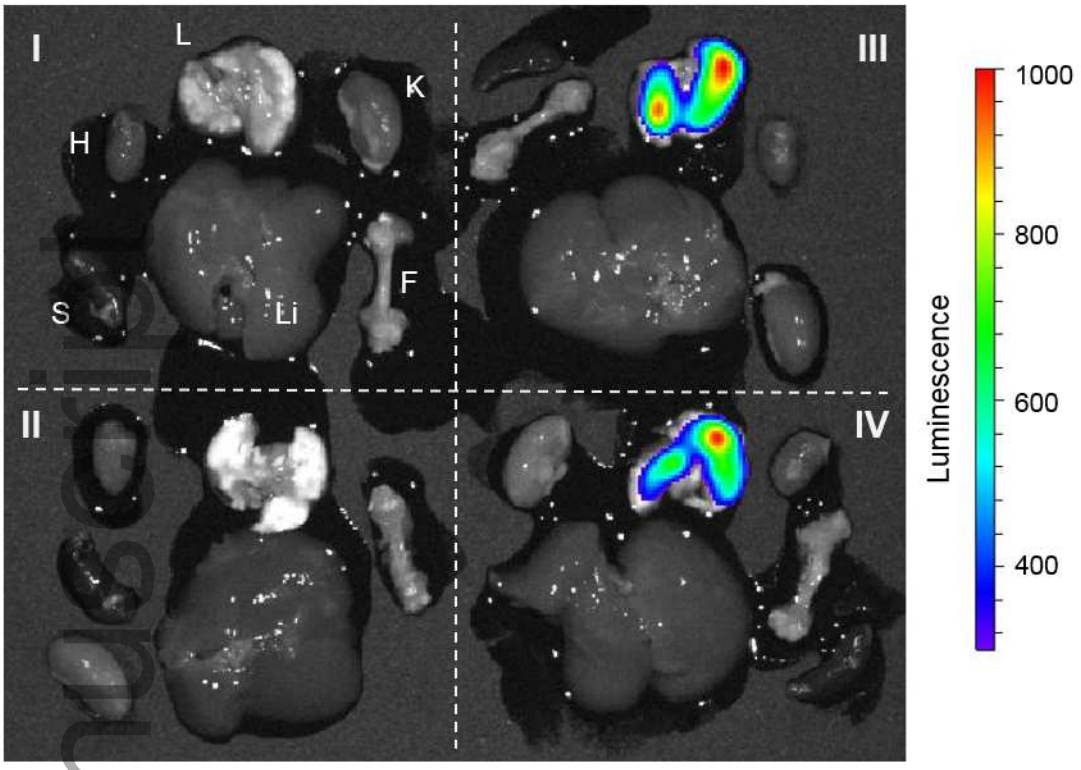

I) healthy; II) iVPC intracardial injected; III) targ-iVPC; and IV) non-targ-iVPC

micc_12493_f6.png